CELLULAR AUTOMATA FINITE ELEMENT (CAFE) MODELLING OF TRANSITIONAL DUCTILE-BRITTLE FRACTURE IN STEEL

A. Shterenlikht[1] and I. C. Howard[2]
[1] Materials Science Centre, Manchester University, Grosvenor Street, Manchester, M1 7HS, UK
[2] Mechanical Engineering Department, Sheffield University, Mappin Street, Sheffield, S1 3JD, UK
a.shterenlikht@umist.ac.uk, i.howard@sheffield.ac.uk

Abstract

A combination of cellular automata (CA) and finite element (FE) techniques provide a fast and flexible tool for multi-scale modelling of fracture. Two CA arrays with different cell sizes independent of the FE size were created to simulate the ductile and the brittle fracture propagation separately. The FE mesh size is then no longer tied with microstructure but rather chosen to adequately represent the macro strain gradients. Such a CA-FE model is very fast compared with the pure FE local approach modelling of fracture. Moreover both the ductile and the brittle fracture mechanisms can be implemented simultaneously in one run. A progressive step-by-step brittle crack propagation in the Charpy sample was simulated. Good agreement was obtained between the experimental and modelled Charpy energy, percentage of crystallinity and lateral expansion. The model was able to reproduce the scatter in the transition region.

Introduction

Despite considerable success of the local approach to fracture, Howard *et. al.* [1], there are two fundamental problems inherent in this technique that significantly restrict its usage in modelling transitional ductile-brittle fracture. Both problems have their roots in the complex inhomogeneous nature of materials such as steels and in the limitations of the finite element approach. The first problem is the high computational cost due to large numbers of small finite elements. Conflicting demands for the mesh size due to the different physical nature of ductile and brittle fracture is the second.

The Cellular Automata – Finite Element (CAFE) approach used in this work offers solution to both problems, Shterenlikht [2]. In this approach material properties are moved away from the finite element mesh and distributed across the appropriate number of cellular automata arrays (CA arrays). Thus a finite element mesh is designed only to represent the macro strain gradients adequately. This is now a solely structural entity. A number of CA arrays, in which cell sizes can be chosen independently, provide the means to analyse material properties at each size scale separately. So a CAFE model can accommodate as many size scales as necessary to address all material properties of interest. However only two CA arrays are required to model the transitional ductile-brittle fracture.

The CAFE model

The CAFE model was realised via the user material subroutine VUMAT in the Abaqus Explicit finite element code [3]. This program utilises explicit dynamic integration of the equations of motion. Reduced integration 8-node finite elements were used to mesh the anticipated damage zone. These elements have only one integration point.

A number of local models for ductile damage exist, of which the most widely used are the Gurson[4, 5] model and that of Rousselier [6, 7]. The CAFE model reported here uses the Rousselier model to represent the development of ductile damage, principally because of its combination of simplicity and realism. However, comparable results could be obtained by encoding the Tvergaard [5] modified Gurson [4] model.

Two independent CA arrays, called hereafter *the brittle CA array* and *the ductile CA array*, were created. The cell size in the brittle CA array is related to a size scale characterisic of brittle fracture. Accordingly the ductile CA array cell size is related to some characteristic distance relevant in ductile fracture.

The general structure of the CAFE model is shown in Fig. 1.

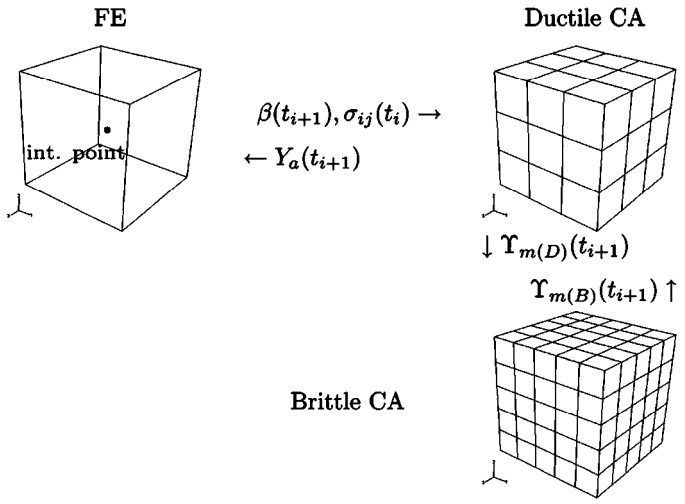

FIGURE 1. Flow of information between the finite element integration point and the ductile and the brittle CA arrays.

At each time increment, t_{i+1}, the Rousselier model integration is performed at the finite element integration point producing the new FE stress tensor, $\sigma_{ij}(t_{i+1})$, and the new damage variable, $\beta(t_{i+1})$. The new damage variable is fed to the ductile CA array and distributed across all ductile CA cells according to the local strain concentration associated with any dead cells (microvoids). The FE stress tensor from the previous time increment, $\sigma_{ij}(t_i)$, is used to calculate the maximum principal stress and its direction cosines. These direction cosines define planes in which fracture propagation is most likely.

Each ductile CA cell is assigned a randomly generated critical value of the damage variable at the beginning of the simulation. Thus a simple ductile fracture criterion can be formulated. A ductile CA cell “dies” when its damage variable exceeds the critical value for this cell. The analysis of the ductile CA array therefore only consists of checking all ductile CA cells against this fracture criterion. This is a very fast procedure.

After all ductile CA cells have been processed, the state of the ductile CA array, $\Upsilon_{m(D)}$, is mapped over the brittle CA array because the two arrays occupy the same physical space and any change of state in one array has to be visible in the other array.

The simulation of fracture propagation at the brittle CA array is slightly more complicated than at the ductile array. Each brittle CA cell is assigned a randomly generated grain size, d,

and grain orientation angle, θ, at the beginning of the analysis. The fracture stress for this cell is calculated as follows, Lin *et al.* [8]:

$$\sigma_F = [\pi E \gamma_p/(1-\nu)2d]^{1/2} \quad (1)$$

where E is Young's modulus, is ν Poisson's ratio and γ_p is the effective surface energy. Wu et al. [9] showed that the fracture stress calculated with equation (1) using coarse grains sizes correlates well with that measured experimentally for a Nb-microalloyed thermomechanically controlled rolled (TMCR) steel.

The maximum principal stress is distributed across all brittle CA cells according to the local strain concentration. The fracture will propagate from a dead brittle cell m to a neighbouring cell l if the maximum principal stress at cell l exceeds its fracture stress and the misorientation angle between these two cells, $|\theta_m - \theta_l|$ is smaller than the misorientation threshold, θ_F. Such a criterion is based on experimental results reported by Nohava et al. [10] and Bhattacharjee and Davis [11], which show that grain boundaries with high grain misorientation angles might inhibit or even stop brittle fracture. It is assumed that θ_F is temperature dependent by analogy with the temperature dependence of the parameters of the Beremin model for cleavage. Burstow [12] has found that the best fitted values for the reference stress, σ_u, of the Beremin model change significantly with temperature in a model in which the Weibull modulus, m, was insensitive to temperature.

The use of only one grain orientation angle is, of course, a modelling simplification. In principle two angles are required to describe a crystal orientation. However, what really matters in modelling crack propagation from one grain to another is the grain misorientation angle, that is the minimum of all angles formed by pairs of crystallographic planes, where each pair contains one crystallographic plane of one grain and one crystallographic plane of the other grain. Perhaps it would be more correct to call θ a grain orientation angle class or type.

At present fracture nucleation is not explicitly modelled. It is assumed that some brittle CA cells contain cleaved grain boundary carbides which may act as brittle fracture nucleation sites. The fraction of such cells is one of the model parameters.

Similarly to the ductile CA array the brittle fracture analysis is performed by assessing all brittle CA cells against the brittle fracture criterion described above. After all brittle CA cells have been processed the state of the brittle CA array, $\Upsilon_{m(B)}$, is mapped onto the state of the ductile CA array to synchronise their states, Fig. 1.

Finally the state variables of the FE integration point, $Y_a(t_{i+1})$, are calculated and returned back to the FE solver. At present there are two state variables: integrity, that is the fraction of alive cells, and the percentage of the brittle phase, that is the ratio of the number of dead brittle cells to the number of dead ductile cells. If integrity falls below a certain limit the FE integration point is considered failed and the fracture is assumed to cross the whole of the finite element.

Experiment

The CAFE model introduced above was used to simulate the Charpy impact test of a TMCR steel. The finite element mesh used is shown in Fig. 2. Only finite elements located at or near the anticipated crack propagation path were modelled with the CAFE approach, the

rest were pure finite elements. The specimen, the anvils and the striker were meshed and the contact interactions with friction were defined.

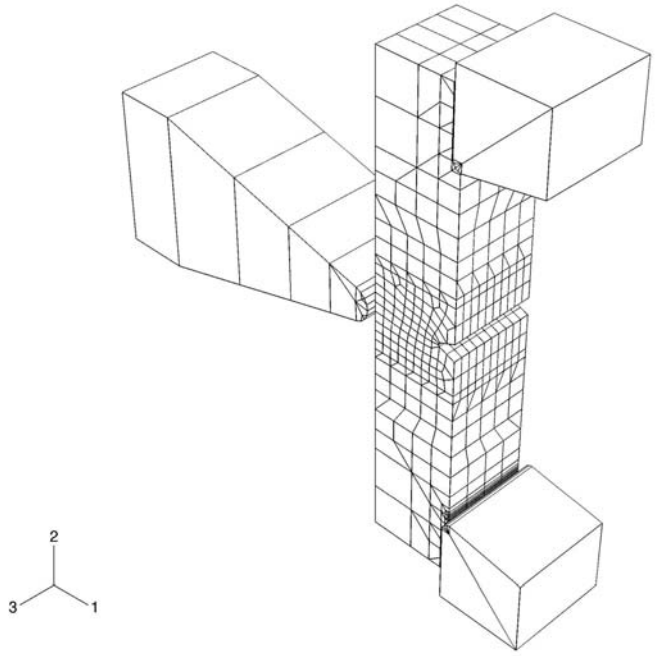

FIGURE 2. The finite element mesh of the Charpy specimen, the anvils and the striker.

The ductile cell size was taken as 0.2 mm based on the spacing between larger dimples, Fig. 3a, which for this TMCR steel are probably associated with larger precipitates, Davis [14]. Accordingly the brittle cell size was taken as 0.1 mm based on the cleavage facet size, Fig. 3b. Thus each finite element in the damage zone was associated with 125 ductile and 1000 brittle CA cells. The whole of the damage zone, which consisted of 900 FEs had, therefore, 900000 brittle and 112500 ductile CA cells. It is worth noting that a pure FE model with such high numbers of FEs would be very difficult, if at all possible, to run except on a dedicated supercomputer. In contrast, the running time of such a CAFE Charpy test model was 2 days on a Pentium III 1GHz PC.

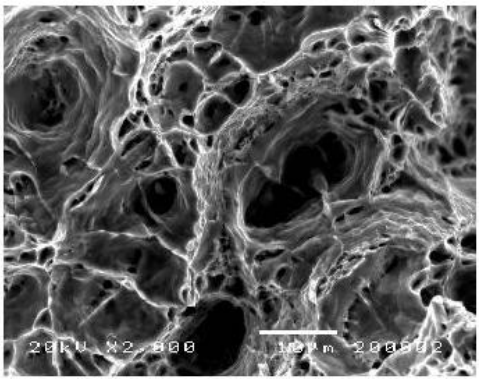

a. Ductile fracture

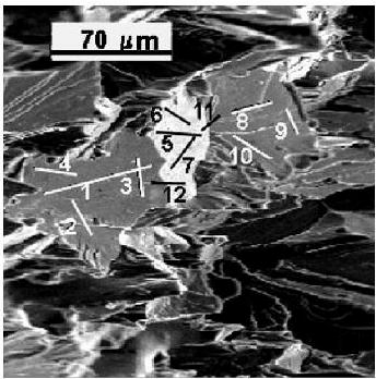

b. Brittle fracture

FIGURE 3. Typical ductile and brittle fracture surfaces of the TMCR steel modelled. Fig. a. courtesy of Davis [14], Fig. b. is reproduced from [11].

Results

Fig. 4 shows a crack propagating through the Charpy sample at several time instances. Figs. 4a and 4b show the initial ductile crack growth (green colour) from the root of the notch. The brittle fracture (black colour) starts after some ductile crack growth, Fig. 4c, and continues until the remaining ligament is very small, Fig. 4g, and the final fracture is due to plastic collapse. The final fracture surface shows a brittle zone surrounded by a ductile region, Fig 4h.

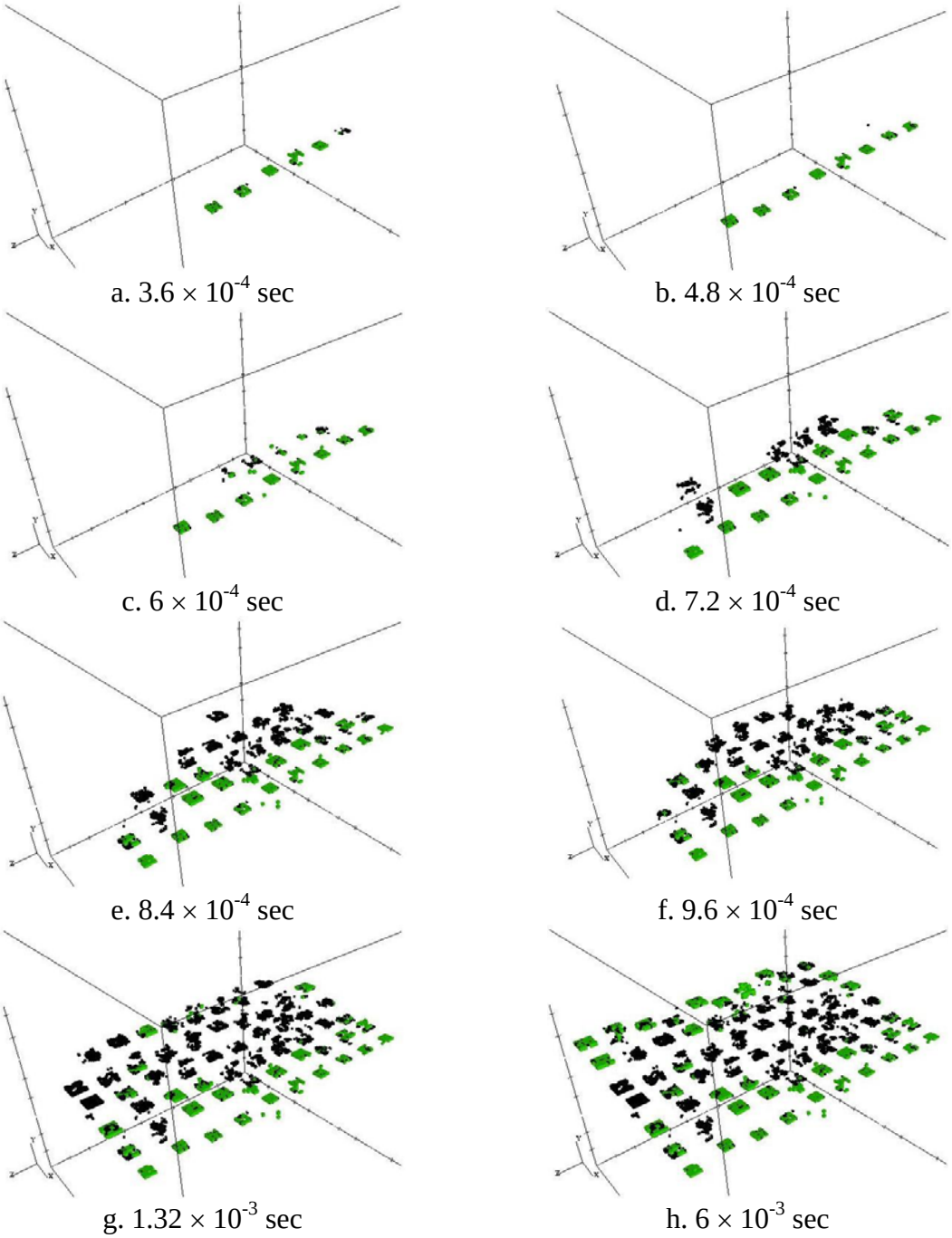

a. 3.6×10^{-4} sec b. 4.8×10^{-4} sec

c. 6×10^{-4} sec d. 7.2×10^{-4} sec

e. 8.4×10^{-4} sec f. 9.6×10^{-4} sec

g. 1.32×10^{-3} sec h. 6×10^{-3} sec

FIGURE 4. Fracture propagation on the CA scale at –30^{o}C. Only dead brittle (black) and dead ductile (green) cells are shown.

The fracture surface obtained in another simulation is compared with the experimental one in Fig. 5. The locations and shapes of the brittle zones are in a qualitative agreement.

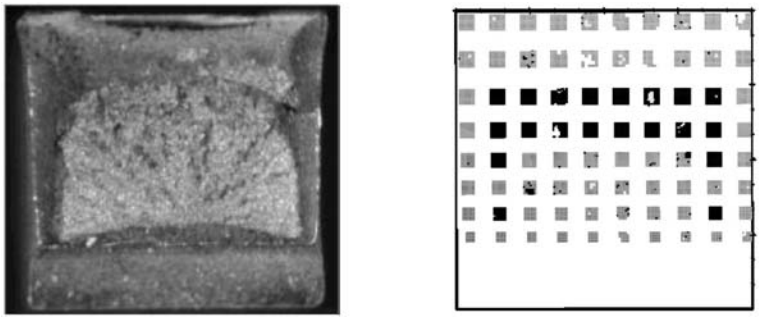

a. Experiment b. Simulation

FIGURE 5. Experimental (a) and simulated (b) Charpy fracture surfaces. In (b) the black colour denotes brittle fracture and grey, the ductile fracture.

Transition data was obtained by running the model at temperatures from –80°C to 0°C, three times at each temperature. Fig. 6 shows the simulated percentage of the brittle phase and total energy absorbed in the test. Overall there is a good agreement between the model and the experimental data. However, the model predicted a 50% ITT at approximately –30°C whereas the experimental ITT is –50°C – 60°C.

The model predicts energies in excess of 50J at the lower shelf where the fracture is 100% brittle. This unrealistic result is caused by the fact that at present a crack cannot cross from one FE to another due to the limitations in the Abaqus code. As a consequence the crack has to reinitiate in each FE. This, of course, requires additional energy, raising the lower shelf toughness to unrealistic values.

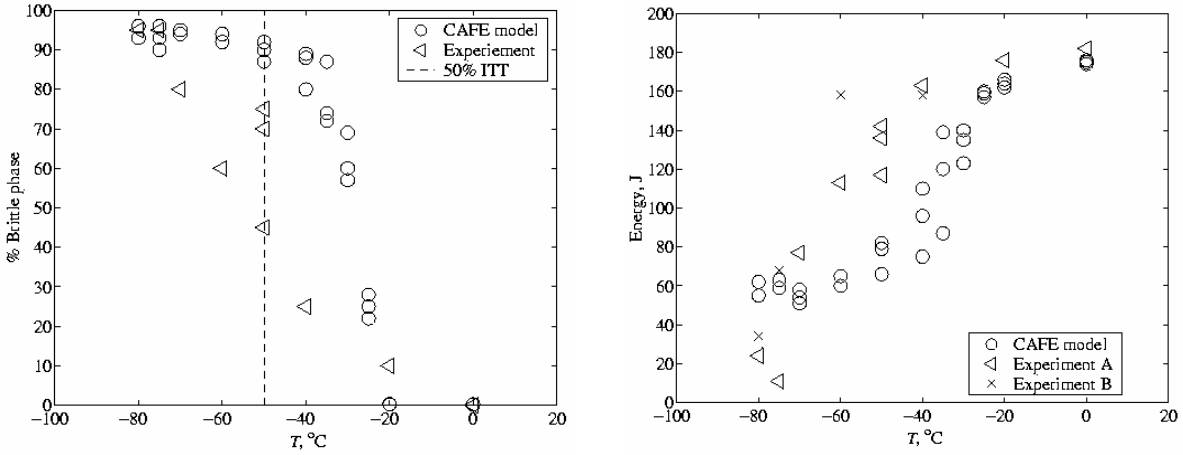

FIGURE 6. Percentage of brittle phase and transition Charpy energy data. The 50% ITT and experimental data A are taken from Bhattacharjee et al. [13]; the experimental brittle phase was provided by Corus UK Ltd and the experimental data B is courtesy of Davis [14].

The lateral expansion predicted by the model also agrees well with that measured by a calliper as shown in Fig. 7.

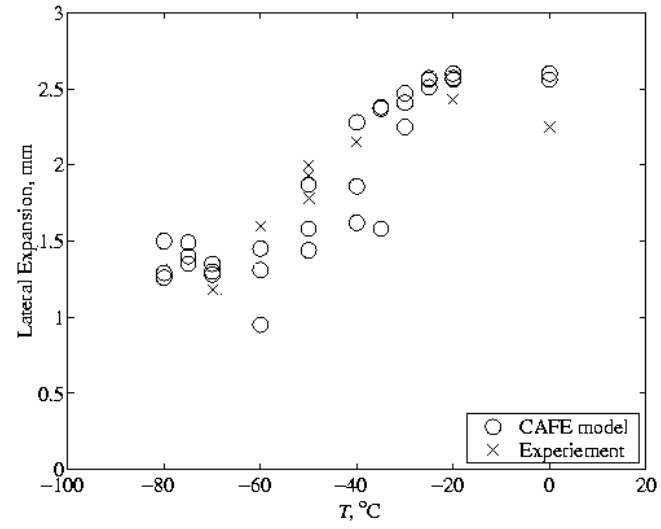

FIGURE 7. Simulated and experimental Charpy lateral expansion data.

Discussion

The use of random number generators for grain size, grain orientation angle and the critical value of the damage variable means that during each modelling run the crack will propagate through a unique arrangement of CA cells. Thus it is possible to reproduce experimental scatter at both the micro (CA) and the macro (FE) scales. Figs. 4h and 5 show that two model runs generated two different fracture surfaces at the transition temperature –30^{o}C. On the other hand Figs. 6 and 7 show that the scatter in the transition region results predicted by the model is higher that at the lower and at the higher shelf. This is consistent with the experimental data.

Since CAFE model simulates progressive brittle fracture propagation, it differs fundamentally from the weakest link models (e.g. Beremin [15], Ruggieri [16]) in which the onset of brittle fracture is the critical event. Weakest link models typically assume that when the probability of brittle fracture exceeds a certain threshold the crack propagates in an unstable manner right through the structure under analysis. Neither the location of the cleavage initiation point, nor the shape of the brittle region, nor crack arrest can be predicted by these weakest link models. In contrast the CAFE model is suitable for such analysis.

Conclusions

The CAFE model used in this work has proven to be suitable for full three-dimensional multi-scale modelling of fracture. The model is fast, stable, flexible and expandable. The level of microstructural detail included is limited only by the experimental data available. For example, if statistics on carbide inclusions are available, they can be easily introduced into the model by adding another CA array with cell sizes relevant to carbide inclusion size. The ductile and the brittle fracture modes can be “switched” on and off, so the model parameters for both fracture mode can be calibrated independently.

Plans for the immediate future include finding ways to simulate crack propagation across the FE boundary. This will make model performance at the lower shelf more realistic.

References

1.Howard, I. C., Li, Z. H. and Sheikh, M. A., In *Fatigue and Fracture Mechanics: 30th Volume,* edited by P. C. Paris and K. L. Jerina, ASTM, Philadelphia, USA, 2000, 152-168.

2.Shterenlikht, A., PhD Thesis, Mechanical Engineering Department, The University of Sheffield, 2003.

3.HKS, *Abaqus Theory Manual,* Hibbitt, Karlsson & Sorensen, Inc., Providence, Rhode Island, USA, 2001.

4.Gurson, A. L., *J. Eng. Mat. and Technology,* vol. 99, 2-15, 1977.

5.Tvergaard, V., *Int. J. Fract. Mech.,* vol. 17, 389-407, 1981.

6.Rousselier, G., Devaux, J. C., Mottel, G. and Devesa, G., In Nonlinear Fracture Mechanics: Volume II – Elastic Plastic Fracture, edited by J. D. Landes, A. Saxena and J. G. Merkle, ASTM, Philadelphia, USA, 1983, 332-354.

7.Rousselier, G., *Nuclear Eng. Design,* vol. **105**, 97-111, 1987.

8.Lin, T., Evans, A. G. and Ritchie, R. O., *Met. Trans.,* vol. 18A, 641-651, 1987.

9.Wu, S. J., Davis, C. L., Shterenlikht, A. and Howard, I. C., *to be submitted to Met. Trans.,* 2004.

10.Nohava, J., Hausild, J. P., Karlik, M. and Bompard, P., *Mat. Characterization,* vol. 49, 211-217, 2002.

11.Bhattacharjee, D. and Davis, C. L., *Scripta Mat.,* vol. 47, 825-831, 2002.

12.Burstow, M. C., Int. J. Pres. Ves. Piping, vol. 80, 797-805, 2003.

13.Bhattacharjee, D., Davis, C. L. and Knott, J. F., Ironmaking and Steelmaking, vol. 30, 249-255, 2003.

14.Davis, C. L., Private Communication. Metallurgy and Materials, The University of Birmingham, UK.

15.Beremin, F. M., *Met. Trans.,* vol. 14A, 2277-2287, 1983.

16.Ruggieri, C., *Prob. Eng. Mech.,* vol. 13, 309-319, 1998.